

Environmental Science Processes & Impacts

Accepted Manuscript

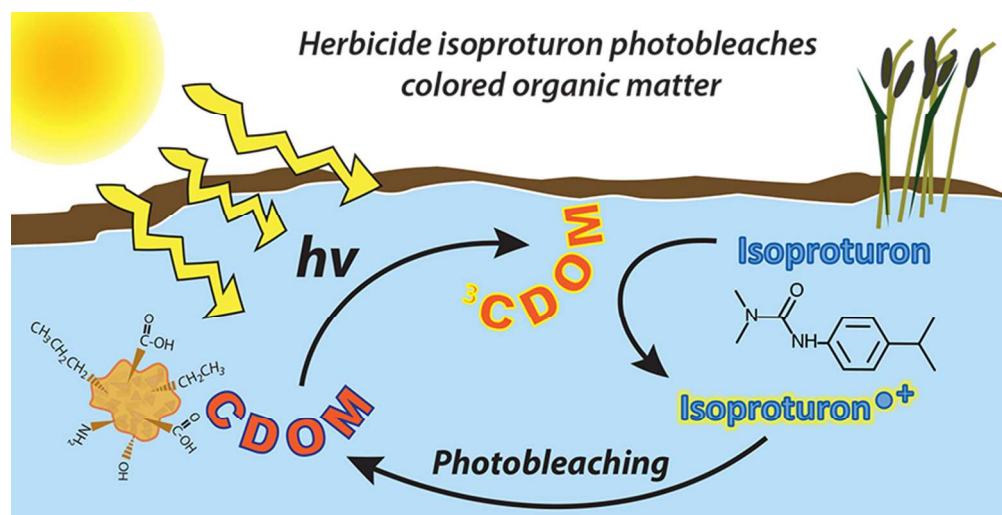


This is an *Accepted Manuscript*, which has been through the Royal Society of Chemistry peer review process and has been accepted for publication.

Accepted Manuscripts are published online shortly after acceptance, before technical editing, formatting and proof reading. Using this free service, authors can make their results available to the community, in citable form, before we publish the edited article. We will replace this *Accepted Manuscript* with the edited and formatted *Advance Article* as soon as it is available.

You can find more information about *Accepted Manuscripts* in the [Information for Authors](#).

Please note that technical editing may introduce minor changes to the text and/or graphics, which may alter content. The journal's standard [Terms & Conditions](#) and the [Ethical guidelines](#) still apply. In no event shall the Royal Society of Chemistry be held responsible for any errors or omissions in this *Accepted Manuscript* or any consequences arising from the use of any information it contains.



78x40mm (300 x 300 DPI)

Environmental Impact Statement:

This contribution examines the role of herbicides on the alteration of chromophoric dissolved organic matter (CDOM) by sunlight in wetland surface waters. Our paper is the first to show that organic compounds that can undergo oxidation by excited CDOM triplets can also catalyze the destruction of chromophores capable of absorbing photons found in sunlight. We also demonstrated that conventional photolysis experiments conducted in sealed phototubes in simulated or natural sunlight resulted in the depletion of dissolved oxygen within the reactor. Thus, this second phenomenon may have ramifications with respect to how photochemical experiments are designed and executed as well as the data that is generated.

1
2
3
4
5
6
7
8
9
10
11
12

Contaminant-Mediated Photobleaching of Wetland Chromophoric Dissolved Organic Matter

Maureen Langlois[†], Linda K. Weavers[‡], Yu-Ping Chin ^{*§}

[†] Environmental Science Graduate Program, [‡] Department of Civil, Environmental, and Geodetic Engineering, [§] School of Earth Sciences, The Ohio State University, Columbus, OH 43210

*To whom correspondence should be made: Tel. +1-614-292-6953: yo@geology.ohio-state.edu

13
14
15
16
17
18
19
20
21
22
23
24
25
26
27
28
29
30
31
32

Abstract

Photolytic transformation of organic contaminants in wetlands can be mediated by chromophoric dissolved organic matter (CDOM), which in turn can lose its reactivity from photobleaching. We collected water from a small agricultural wetland (Ohio), Kawai Nui Marsh (Hawaii), the Everglades (Florida), and Okefenokee Swamp (Georgia) to assess the effect of photobleaching on the photofate of two herbicides, acetochlor and isoproturon. Analyte-spiked water samples were irradiated using a solar simulator and monitored for changes in CDOM light absorbance and dissolved oxygen. Photobleaching did not significantly impact the indirect photolysis rates of either herbicide over 24 hours of irradiation. Surprisingly, the opposite effect was observed with isoproturon, which accelerated DOM photobleaching. This phenomenon was more pronounced in higher-CDOM waters, and we believe that the redox pathway between triplet-state CDOM and isoproturon may be responsible for our observations. By contrast, acetochlor indirect photolysis was dependent on reaction with the hydroxyl radical and did not accelerate photobleaching of wetland water as much as isoproturon. Finally, herbicide indirect photolysis rate constants did not correlate strongly to any one chemical or optical property of the sampled waters.

33 Introduction

34 Wetlands have the potential to attenuate mobile contaminants transported by runoff
35 associated with agriculture. Relatively long retention times (compared to streams) and a
36 favorable aspect ratio with respect to sunlight exposure make wetlands well suited as
37 photoreactors for contaminant degradation via direct or indirect photolysis. Direct
38 phototransformation of organic contaminants can occur in wetland waters, but many of these
39 substances lack the chromophores capable of absorbing photons present in sunlight. A more
40 likely pathway occurs when sunlight activates other wetland water constituents (photosensitizers)
41 that in turn react with contaminants via indirect photolytic pathways. These photosensitizing
42 species include nitrate/nitrite, iron and chromophoric dissolved organic matter (CDOM), which
43 lead to the formation of reactive oxygen species (ROS) such as the hydroxyl radical (OH•),
44 singlet oxygen ($^1\text{O}_2$), and superoxide ($\text{O}_2^-/\text{HO}_2^-$) as well as other excited species including triplet-
45 excited state dissolved organic matter (^3DOM) and organic radicals. These species are unstable
46 and quickly react with other water constituents including DOM (which includes CDOM and non-
47 chromophoric molecules), carbonate species, water, and contaminant molecules.

48 Photobleaching, i.e., the alteration of CDOM composition by both direct and indirect
49 photolysis, is an important physicochemical process in wetland chemistry and contributes to the
50 cycling of organic matter in watersheds. For this reason, CDOM is depleted in sunlit waters more
51 rapidly than DOM in general (1-4). Over time, sunlight exposure decreases the average size of
52 DOM molecules, measured both in terms of lower molecular weight and changes in light
53 absorbance (5). In wetlands the processing of DOM into smaller components has been attributed
54 more to photolytic than microbial processes (6) and has been shown to affect the subsequent
55 bioavailability of DOM to heterotrophic microorganisms (7-9).

56 The extent to which CDOM photobleaching influences the transformation of organic
57 contaminants depends on the chemical and optical properties of the wetland in addition to its
58 hydrology, location, and morphology. Attempts have been made to model these processes using
59 the chemical (10-12) and optical (13, 14) properties of the surface waters, but much is still
60 unknown about the responsible pathways, particularly in wetlands (15-18). Finally, recent
61 research has demonstrated that DOM can inhibit the transformation of contaminants known to
62 react readily with ³DOM (19, 20). One implication of these studies is the possibility that
63 contaminant molecules can act as reactive species capable of *transforming* CDOM in irradiated
64 waters, which to our knowledge has not previously been explored.

65 For this study we investigated 1) the role of various wetland water chemical constituents
66 and DOM optical characteristics on the photodegradation of two herbicides isoproturon (IP) and
67 acetochlor (AC), and 2) the link between contaminant degradation and the coincident CDOM
68 transformation. Both of our target compounds are pre-emergent broadleaf herbicides used in
69 large-scale agriculture and they have chemical properties that make them suitable for use in
70 laboratory studies (low volatility, negligible hydrolysis rates at ambient temperatures, etc.). The
71 objectives of the current study, therefore, are 1) to quantify the rates of change of CDOM and of
72 the probe compound herbicides AC and IP during the course of solar irradiation in various
73 wetland waters, 2) to relate these changes to water chemistry and optical characteristics, and 3)
74 to determine the extent to which light-induced changes in CDOM and in the herbicides are
75 interconnected.

76

77

78

79 **Materials and Methods**

80 *Site descriptions:*

81 Water was collected from four freshwater wetland sites in the U.S. between June 2010
82 and January 2011 to capture the greatest diversity of natural photosensitizers. Yocom Farm
83 wetland, Champaign County, Ohio (YCF) is a small (<1 ha) modified forested wetland receiving
84 tile drainage from corn and soybean fields in central Ohio. Kawai Nui Marsh (KNM) is a
85 restored freshwater marsh on Oahu, Hawaii (335 ha). The Everglades Wildlife Management
86 Area Water Conservation Area 2B (EVG), located near Ft. Lauderdale, FL, is positioned at the
87 upstream end of the Okeechobee/Everglades system that covers much of southern Florida.
88 Samples were taken from a channel emerging from an expansive stretch of vegetated marsh
89 (USGS EDEN station S11A-H, upstream). The Okefenokee Swamp (OKS) is a 1.77×10^5 -ha,
90 peat-filled “blackwater” swamp that is the source of the Suwannee River. Samples were taken
91 from the edge of designated open marsh area accessed from the eastern entrance to the
92 Okefenokee National Wildlife Refuge, Georgia. In all cases, samples were taken from the shore
93 of inundated wetland areas with minimal emergent plant shading. Samples were collected with a
94 glass container on a 3-m extender rod from a depth of 30-50 cm and were vacuum-filtered as
95 soon as possible (< 2 h) with pre-combusted Gelman A/E (1 μ m) glass filters and stored in the
96 dark on ice until being refrigerated at 4°C. In the case of OKS samples, high turbidity of the
97 water necessitated splitting the sample and filtering only half of the sample in the field (split
98 OKS_{FF}) and the remaining half in the lab two days later (split OKS_{LF}).

99 *Water chemical characterization:*

100 Parameters measured in the field at each sampling time include water temperature and
101 dissolved oxygen (YSI EcoSense DO200, YSI Environmental, Inc. Yellow Springs, OH). The

102 pH and conductivity of the filtrate were measured immediately after filtering (Thermo Orion
103 model 130 conductivity meter, Beverly, MA). Laboratory characterization of the samples
104 included UV-visible (UV-Vis) absorbance (Varian Cary 13 UV-visible spectrophotometer,
105 Agilent Technologies, Santa Clara, CA, U.S.A.), dissolved organic carbon (DOC) analysis
106 (Shimadzu TOC-V CPN, Columbia, MD, U.S.A.), total iron (Varian Vista AX CCD ICP-AES,
107 Agilent Technologies, Santa Clara, CA, U.S.A.) and inorganic ions (Dionex DX-120, Sunnyvale,
108 CA, U.S.A. and Skalar San++ Nutrient Analyzer, Breda, Netherlands).

109 *Optical characterization of water samples:*

110 UV-visible absorbance values were corrected for the absorbance of water (Millipore
111 Milli-Q water purification system, Billerica, MA). Specific UV absorbance ($SUVA_{254}$) values
112 were calculated in the manner of (21) using equation (1),

$$113 \quad SUVA_{254} = A_{254} / [DOC] \quad (1)$$

114 where A_{254} is the absorbance of the wetland water at $\lambda = 254$ nm measured in a 1 cm path-length
115 cuvette and [DOC] is expressed in moles C per L (M) and/or mg C per L (mg-C/L). Samples
116 were diluted if their absorbance were greater than 1 and DOC was re-measured for the diluted
117 samples.

118 To calculate spectral slope, Napierian absorption coefficients for $\lambda = 250$ -500 nm were
119 calculated as follows for each water,

$$120 \quad a_{\lambda} = (2.303 A_{\lambda}) / l \quad (2)$$

121 where a_{λ} = the absorption coefficient (m^{-1}) at λ , A_{λ} = corrected UV-visible absorbance at λ , and l
122 = path length (1 cm for our instrument). A plot of $\ln a$ as a function of λ yields a relatively linear
123 curve whose slope (S) in various ranges were determined; here $S_{275-295}$, $S_{350-400}$ and S_R , the ratio
124 of $S_{275-295}/S_{350-400}$ were calculated in the manner of Helms *et al.* (5).

125 Absorbance was also used to calculate a screening factor (SF) for each water sample.

126 Briefly, SF at any given λ is calculated as follows,

$$127 \quad SF = (1 - 10^{-A}) / (2.303AI) \quad (3)$$

128 where the variables are the same as defined above. SF is plotted as a function of wavelength and
129 fitted to a fourth-order polynomial ($R^2 > 0.98$), which is then integrated over the wavelengths of
130 interest and subtracted from the value without light screening (22).

131 *Photolysis experiments:*

132 Herbicides were obtained from Chem Service (West Chester, PA) at the highest available
133 purity. Wetland water samples were adjusted to the field-measured pH using HCl or NaOH of
134 highest available grade (iron free), spiked with aqueous stock solutions of IP or AC to form a 5
135 μM reaction solution, and stirred open to air at room temperature for 2-3 hours. Fulvic acid
136 solutions containing Suwannee River or Pony Lake fulvic acids (SRFA or PLFA) were prepared
137 at pH 8 in a 1 mM bicarbonate solution.

138 Quartz photoreaction tubes (path length = 0.9 cm, volume = 8 mL) were filled with
139 reaction solution and sealed with airtight caps in the dark. Reactors were irradiated in a solar
140 simulator fitted with a collimating lens (Suntest CPS+, Atlas MTT LLC, Chicago, IL). Samples
141 were irradiated for at least one half-life for both analytes. Dark controls consisted of foil-
142 wrapped tubes were placed concurrently within the solar simulator. Direct photolysis rates were
143 determined by irradiating analyte solutions in the absence of DOM and other photosensitizers.

144 Overall light intensity of the solar simulator was determined using both *p*-
145 nitroanisole/pyridine and *p*-nitroacetophenone /pyridine actinometry (23), which is calibrated to
146 the known quantum yield of the reaction at 313 and 366 nm. The light emitted by our solar
147 simulator (on the manufacturer's 550 W/m² setting) was determined to be ~ 2.0 times as strong

148 as the summer sun at 40°N latitude (24). Irradiance over the course of experiments was
149 continuously monitored using a UV-light radiometer (VWR International, Bridgeport, NJ) that
150 integrates signal over $\lambda = 320\text{-}390$ nm. The temperature of the solar simulator was maintained at
151 $27 \pm 3^\circ\text{C}$.

152 For a subset of photolysis experiments, UV-Vis absorbance and dissolved oxygen (DO)
153 were measured at time-points during irradiation. DO was determined using a micro-DO probe
154 (Lazar Research Laboratories, Inc., Los Angeles, CA) dry-calibrated in air and wet-calibrated
155 using air-saturated water. DO was measured in most cases within 1 hour of removal from the
156 solar simulator and after the tubes had equilibrated to room temperature. Influx of atmospheric
157 O_2 into the tubes during measurement was determined to be minimal during initial readings
158 (acquisition time 2-3 min), but interfered with measurements over longer spans of time,
159 precluding multiple readings of each sample tube. Herbicide concentrations were analyzed using
160 a Waters reversed-phase HPLC (Milford, MA) equipped with a Nova-Pak C18 column (3.9 x
161 150 mm). With a mobile phase of 55:45 ACN:H₂O (v:v), detection parameters were as follows:
162 for IP, $\lambda = 240$ nm, retention time. ≈ 4.7 min; and for AC, $\lambda = 220$ nm, retention time ≈ 6.5 min.

163 We made amendments to the indirect photolysis experiments with EVG samples to
164 elucidate reaction mechanisms. To assess the role of OH^\bullet , *t*-butanol was added to EVG water
165 spiked with AC such that the final concentrations were 25 mM and 5 μM , respectively. Another
166 set of mechanistic experiments involved bubbling EVG with argon (1 min/mL solution) to
167 displace atmospheric gases and then preparing photolysis solutions in a glovebox filled with
168 N_2/H_2 (95%/5%). Initial readings on these low- O_2 solutions showed that this treatment yielded
169 DO of 35-40% of atmospheric O_2 saturation.

170

171 *Kinetic Modeling:*

172 The observed rate of loss in complex mixtures such as natural waters is attributed to both
173 direct and indirect photolysis. To determine the rate constant that describes direct photolysis
174 occurring in a given wetland water (k_{dir}), the rate constant for direct photolysis in water was
175 multiplied by the appropriate screening factor (Table 1). Indirect reaction rate constants (k_{ind})
176 were then calculated by subtracting k_{dir} from k_{obs} (equation [4]),

$$177 \quad k_{ind} = k_{obs} - k_{dir} \quad (4)$$

178 where k_{obs} is the overall rate constant from each experiment.

179 **Results**

180 *Chemical and optical characteristics of wetland waters:*

181 The four wetlands sampled in this study represent a broad range of chemical composition,
182 from the relatively low-DOC, moderately alkaline YCF to the turbid, acidic OKS (Table 1). The
183 heterogeneity of CDOM composition precludes a simple chemical quantification of the colored
184 fraction presumed to dominate photochemical activity. Accordingly, UV-visible absorbance
185 spectra for each water sample were used to indirectly characterize CDOM optical properties.
186 Screening factors for all sampled waters aligned inversely with [DOC], with the highest [DOC]
187 sample (OKS_{LF}) absorbing nearly 50% of ambient sunlight (Table 1). $SUVA_{254}$ values (an
188 estimate of aromaticity) of the wetland waters fell roughly into two categories, with YCF and
189 EVG at $\sim 360 \text{ M}^{-1} \text{ cm}^{-1}$ ($\sim 2.95 \text{ L mg C}^{-1} \text{ m}^{-1}$) and KNM and OKS_{FF} at $\sim 225 \text{ M}^{-1} \text{ cm}^{-1}$ ($\sim 1.85 \text{ L mg}$
190 $\text{C}^{-1} \text{ m}^{-1}$). High aromaticity has been reported in the northern Everglades previously (25).

191 *Changes to CDOM during light exposure:*

192 During the course of irradiation experiments in the solar simulator, EVG and OKS water
193 samples were periodically monitored for UV-visible absorbance and DO. In all cases, the

194 absolute UV-Vis absorbance of the samples decreased with light exposure, indicating loss of
195 chromophores over time. This trend is consistent with numerous previous observations of
196 photobleaching (1, 6, 8).

197 $S_{275-295}$ increased steadily with light exposure for all waters tested, implying greater loss
198 of absorbance at the higher λ (lower energy) end of this range (Table 2). Increases in $S_{275-295}$ for
199 our samples corroborate previous studies of photobleaching in natural waters and is indicative of
200 the production of lower molecular weight moieties (5, 26). While $S_{275-295}$ changed at similar rates
201 among measured waters (mean rate of change = $1.39 \times 10^{-3} \text{ hr}^{-1}$), the $S_{350-400}$ parameter was more
202 variable (Table 2). Helms et al., (5) also observed both phenomena for various DOM samples
203 with increasing $S_{275-295}$ as a function of irradiance and variability in $S_{350-400}$.

204 Water samples spiked with AC or IP (5 μM) affected the rate of spectral slope change
205 during the irradiation of EVG water (Table 2). Dark controls showed that the initial spectral
206 slopes for EVG water in the presence and absence of the herbicides were identical, indicating
207 that the contribution of analyte light absorbance to the total absorbance of the sample is
208 negligible. Further, the presence of each herbicide caused a different effect on spectral slope
209 with time. With AC, $dS_{275-295}/dt$ and $dS_{350-400}/dt$ changed slightly compared to no herbicide;
210 however, the slope ratio S_R remained constant. By contrast, the presence of IP considerably
211 accelerated the rate at which $S_{350-400}$ decreased, causing a rate of change of S_R *over twice* that of
212 no-herbicide or AC-containing solutions. Therefore, the presence of herbicides alters the way in
213 which the CDOM changes over the course of irradiation. We believe that this has not been
214 observed in previous DOM mediated herbicide photodegradation studies.

215 Reducing the initial DO concentration to sub-oxic levels (defined here as argon purged
216 solutions) in our experiments slightly lowered the rate of change in $S_{275-295}$, for AC spiked

217 solutions perhaps implying that photobleaching of chromophores absorbing lower-wavelength
218 photons is more due to direct photolysis as oppose to the presence of reactive oxygen species.
219 The opposite occurred for the rate of change in $S_{275-295}$, for IP spiked solutions whereby we
220 observed a slight increase. Additional experiments would be necessary to determine the effects
221 of low- O_2 conditions in the presence of herbicides. Our results corroborated those reported by
222 Gao and Zepp (27), who observed some photobleaching in anoxic Satilla River water.

223 In OKS water, all experiments were performed in the presence of herbicides. Compared
224 to irradiation with AC, for both OKS_{FF} and OKS_{LF} the presence of IP resulted in more rapid
225 absorbance changes than those observed in EVG (Table 2). In both OKS splits, the presence of
226 IP caused dS_R/dt to double relative to AC. The factor of two increases in S_R rate of change
227 caused by the presence of IP was consistent among EVG, OKS_{FF} and OKS_{LF} waters *despite* their
228 disparate water characteristics.

229 *Changes in oxygen levels during light exposure:*

230 Irradiated EVG and OKS waters were monitored for changes in DO over the course of
231 irradiation (Table 2). O_2 is a participant in many known indirect photolysis reaction pathways
232 including the photobleaching of CDOM (4, 9), the formation of singlet oxygen (28) and photo-
233 Fenton reactions (29) such that photobleaching has been shown to be largely due to indirect
234 photo-oxidation. From a starting value of 100% atmospheric saturation, we observed steady
235 decreases in DO during all irradiation experiments relative to dark controls. Further, the rate of
236 DO loss was relatively consistent for each water sample over successive trials.

237 Changes in spectral slope in the presence of AC or IP were mirrored by accelerated DO
238 loss relative to wetland water in the absence of the analytes (Table 2). With AC, DO decreased
239 ~30% faster than in wetland water alone, while changes in the presence of IP, the effect was even

240 larger (~70%). Experiments conducted in EVG water under low-O₂ conditions resulted in little
241 change in DO level over the course of the irradiation, although readings exhibited a greater
242 standard deviation compared to air-saturated irradiations. The rate of DO loss was correlated to
243 both DOC and total iron (Fe_{tot}) for the wetland waters, consistent with direct and Fenton-
244 mediated photo-oxidation (Figure 1).

245 For all waters, the presence of IP caused substantially (1.3 to 2.5 times) higher rates of
246 DO loss compared to AC. This enhancement mirrors the increased photobleaching of waters
247 containing IP versus AC described above. Interestingly, the same pattern emerges in the
248 dependency of DO loss rate on DOC and Fe_{tot} shown in Figure 1 *i.e.*, twice the DO loss per unit
249 DOC or Fe_{tot} occurred for solutions containing IP versus AC.

250 *Rates of contaminant loss during light exposure:*

251 *Direct photolysis.* The rates of direct photolysis of AC and IP were measured by
252 irradiating the herbicides in water. The direct photolysis reaction rate constant for AC in water
253 was $7.5 \pm 0.6 \times 10^{-3} \text{ hr}^{-1}$ (half-life: ~ 3.9 d) and is consistent with a previously measured value
254 ($8.2 \times 10^{-3} \text{ hr}^{-1}$) (35). The k_{dir} for IP was smaller at $2.7 \pm 0.9 \times 10^{-3} \text{ hr}^{-1}$ (half-life: ~ 10.6 d). The
255 lower k_{dir} of IP versus AC cannot be explained by their respective absorbance spectra at
256 wavelengths present in sunlight (Figure 2), but is consistent with previous observations (30).

257 *Indirect photolysis.* Observed herbicide loss rate constants (k_{obs}) were measured in
258 irradiated wetland waters (Figure 3) and in buffered fulvic acid solutions. For AC, wetland water
259 accelerated photodegradation over water by a factor of 2-3 even when corrected for light
260 screening (Table 3). Indirect photolysis of AC proceeded with nearly identical k_{ind} for almost all
261 the sampled wetlands (including YCF, KNM, EVG and OKS_{LF}), with a mean of $1.2 \pm 0.1 \times 10^{-2}$
262 hr^{-1} . We also observed increasing k_{ind} for PLFA solutions as DOC concentrations increased (7,

263 14 and 21 mg C/L, pH = 8) whereby the range of k_{ind} is similar to those measured for our wetland
264 samples ($\sim 1.1 \times 10^{-2} \text{ hr}^{-1}$, data not shown). In contrast SRFA solutions (pH = 8) at low (2.5 mg-
265 C/L) concentrations caused little or no enhancement over direct photolysis. One dramatic
266 exception to this pattern was the field-filtered Okefenokee sample (OKS_{FF}) whereby k_{ind} was 4-5
267 times higher than all other waters. All dark controls showed negligible (<1%) herbicide loss.

268 IP photolysis was enhanced by a factor of 30-200 in wetland waters compared to water
269 alone (Table 3). These results agree with previously reported ratios of direct to sensitized
270 photolysis for IP (12). Similar to our observations for AC the irradiation of IP in PLFA solutions
271 with increasing DOC yielded linearly increasing rate constants (Figure 4), consistent with the
272 involvement of ³DOM in IP photolysis as shown by others (12, 30). However, as shown in
273 Figure 4 the correlation between PLFA concentration (as DOC), and IP k_{obs} was not observed for
274 our wetland waters.

275 *Probing mechanisms of indirect photolysis:*

276 *Low-O₂ conditions.* To determine the extent to which O₂ was involved in indirect
277 photolysis, we purged solutions to about 35-40% of atmosphere-equilibrated DO. For AC, low
278 DO conditions did not significantly alter k_{ind} , although deviations from pseudo-first order
279 kinetics occurred (Fig. 3a). For IP, this deviation from pseudo-first order behavior was even
280 more pronounced (Fig. 3b), and the initial rate of degradation was clearly enhanced under low-
281 O₂ conditions.

282 *Addition of t-butanol.* Indirect photolysis for AC was shut down in EVG spiked with *t*-
283 butanol, a known OH• scavenger (Figure 3a). The observed reaction rate constant was actually
284 lower than k_{dir} , suggesting that the quencher shut down the indirect OH• mediated pathway and
285 possibly influence AC. DO loss in the *t*-butanol-spiked solution was lower than an identical

286 solution without the quencher, and more closely approximated the DO loss of EVG water alone
287 (Table 2). Although $dS_{275-295}/dt$ was nearly the same as with non-quenched AC solutions, the S_R
288 rate of change was somewhat lower than even wetland water alone, suggesting some inhibition
289 occurred in photobleaching in the presence of *t*-butanol (Table 2).

290 Discussion

291 *Establishing likely pathways of contaminant degradation:*

292 The herbicides used as probe compounds in this study were chosen because they are
293 known or suspected to have different dominant pathways for indirect photolysis. For AC, no
294 previous data is available for indirect photolysis in sunlit natural waters, but the primary indirect
295 photolytic pathway for other chloroacetanilide herbicides including metolachlor (31, 32),
296 alachlor (16), and propachlor and butachlor (33) involves non-specific ROS species, particularly
297 $OH\cdot$. Our results, using the $OH\cdot$ quencher *t*-butanol (Figure 3a), confirm that this radical is
298 important in AC indirect photolysis in wetland waters.

299 The major formation pathways of $OH\cdot$ in sunlit waters include (1) photolysis of NO_3^- and
300 NO_2^- (2) the reaction of sensitized CDOM with H_2O , and (3) photo-Fenton reactions mediated by
301 Fe (III) and DOM, which becomes important under acidic conditions. Major sinks for $OH\cdot$ are
302 DOM, carbonate, and, to a lesser extent bicarbonate (34). Given the second-order rate constant
303 between AC and $OH\cdot$, ($k_{OH} = 7.5 \times 10^9 \text{ M}^{-1} \text{ s}^{-1}$) (35), a steady state hydroxyl radical
304 concentration ($[OH\cdot]_{ss}$) on the order of 10^{-16} M would be required to achieve the average k_{ind} of
305 $1.2 \pm 0.1 \times 10^{-2} \text{ hr}^{-1}$ that we observed for AC. This is a plausible scenario given that $[OH\cdot]_{ss}$ of
306 this magnitude has been observed in various wetland waters (36).

307 Iron-rich, acidic, highly colored waters such as OKS are known to undergo photo-Fenton
308 $OH\cdot$ production (2, 27), which may help to explain why AC photolysis was three times faster in

309 OKS_{FF} than in any other water. Alachlor, which is structurally similar to AC, was shown to
310 photodegrade much more rapidly in acidified (pH = 4) wetland waters versus unacidified (16),
311 and the same mechanism may be at work with AC. Although OKS_{LF} water was at the same pH
312 as OKS_{FF}, it also had nearly three times the DOC. Both OH• quenching and significant inner-
313 filter effects associated with this high DOC may in part explain the slower AC kinetics in
314 OKS_{LF}. Finally, it is possible that the iron speciation between OKS_{FF} and OKS_{LF} may have also
315 been altered over the intervening two days, which could also affect the reactivity of the two
316 samples.

317 The primary reactive species responsible for IP transformation in natural waters appears
318 to be ³DOM (12, 37) and possibly DOM-derived organic radicals (38), although IP oxidation has
319 been observed with other reactive species including OH• (39). The increased rate of IP
320 photolysis in low-O₂ conditions observed by us corroborates this pathway as dissolved oxygen
321 can compete with IP for ³DOM (Figure 3b). We observed a linear increase in k_{ind} with increasing
322 concentration of PLFA (Table 3, Figure 4) and corroborate the results reported by Gerecke et al.,
323 (12). Surprising there was no linear dependence of k_{ind} on DOC (Figure 4) for any of the wetland
324 waters.

325 We observed no strong correlations between IP k_{ind} and water properties such as
326 absorbance, DOC, or pH, but our results revealed trends. The highest k_{ind} value occurred for
327 EVG (pH = 7.9) while the slowest kinetics was observed for OKS (pH = 3.5). While differences
328 in DOM composition will in part explain our observations these results also support previous
329 findings whereby the rates of triplet-induced degradation increase with pH (37). For example
330 Brucoleri et al., (40) demonstrated that the quantum yield for the formation of triplet DOM
331 increases significantly with increasing pH. Stosser et al., (38) reported a similar phenomenon for

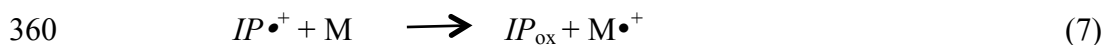
332 the production of organic radicals. The idea that pH is correlated with greater IP
333 phototransformation is supported by Figure 4, whereby the two high-pH water samples with
334 similar SUVA₂₅₄ values (EVG and YCF) fall close to the trend created by PLFA (buffered at pH
335 8). With respect to the influence of DOM composition Guerard et al. (41) observed that
336 photodegradation of the antibiotic sulfadimethoxine (also primarily degraded by ³DOM in
337 sunlight) occurs most quickly in PLFA solution and is not photosensitized by SRFA. We believe
338 that this is partly due to the different antioxidant properties of the fulvic acids whereby the more
339 terrestrially derived SRFA possesses antioxidant poly-phenolic moieties that are not present in
340 PLFA, which is derived from microbial organic matter precursors (20).

341 *Contaminant acceleration of photobleaching with IP:*

342 DOM photobleaching by both direct and indirect photolysis has been attributed to the
343 loss of chromophores. Surprisingly, both AC and IP influenced photobleaching by changing
344 spectral slope and DO beyond the photolytic rates observed in wetland water alone (Table 3). To
345 date we are unaware of any previous study that showed the effect of pesticides on DOM
346 photobleaching. This suggests that the herbicides themselves are involved in the formation of an
347 additional pool of reactive species that can oxidize CDOM. For AC, the change in
348 photobleaching and DO loss compared to solutions in its absence was small. Conversely, IP
349 accelerated the rate of DOM photobleaching substantially. This effect was minimized under low-
350 O₂ conditions, suggesting involvement of DO.

351 We hypothesize that IP and other compounds susceptible to oxidation by triplets may
352 form radical cations ($IP\bullet^+$) through reaction with triplet aromatic ketone moieties in ³DOM as
353 shown in eq. 5 (42, 43). Others have demonstrated that the triplet-sensitized oxidation of
354 phenylureas and other aniline-containing compounds, decreases in the presence of DOM (19,

355 20). The proposed mechanism of this inhibition is DOM-induced reduction of $IP\bullet^+$ back to the
 356 parent IP (eq. 6) as opposed to the continued reaction of $IP\bullet^+$ with other unknown species (M) to
 357 form other products (denoted here as IP_{ox}).



361 Our observation of increased photobleaching of CDOM in the presence of IP is consistent
 362 with reduction of the radical cation $IP\bullet^+$ by CDOM as shown in eq. 6. In high-DOC solutions
 363 OKS_{FF} and OKS_{LF}, the presence of IP increased both spectral changes and consumption of O₂
 364 compared to AC. However, the rate of IP degradation itself is *lowest* in both OKS samples
 365 (Figure 5), which is contrary to the observation that IP reaction rate roughly increases with
 366 increasing DOC (12). The fact that IP increases photobleaching without being rapidly degraded
 367 suggests a pathway similar to eq. 6 as opposed to eq. 7.

368 Our work has identified aspects of these photochemical interactions that merit further
 369 work in order to understand the fate of compounds that predominantly undergo oxidation
 370 through reactive triplets and their possible role in photobleaching. In particular, the role of DOM
 371 chemical composition has not yet been fully investigated. DOM with higher aromatic carbon
 372 moieties is both more likely to inhibit triplet-mediated contaminant oxidation (due to the
 373 presence of naturally occurring anti-oxidant compounds present in the higher plant precursors)
 374 (20) and these substances are more likely to form ¹O₂ (14, 18). Our findings imply that for more
 375 aromatic (allochthonous) DOM, we would expect to see a greater reduction in IP k_{ind} and
 376 possibly a more rapid decrease in DO. Finally, ³DOM moieties may have a range of redox

377 potentials. For example recent studies have suggested the presence of multiple triplet pools with
378 varying susceptibility to reduction by borohydride (18, 42).

379 *Methodological implications of photochemical experimental design:*

380 Changes in DO over the course of a long (8-30 hr) irradiation experiment reveal issues in
381 the application of closed-tube photoreaction experiments. Photochemical experiments often use
382 airtight, capped phototubes (e.g., 16, 44 and others referenced therein). While studies have
383 compared solar simulators and natural sunlight (45, 46), little attention has been devoted to
384 issues regarding the use of sealed phototubes to determine natural water photoreactivity given
385 the potential for artifacts caused by O₂ depletion. Our observations of herbicide degradation
386 kinetics in this study show that later samples deviate somewhat from pseudo-first order kinetics,
387 with more parent compound left than would be predicted by the kinetic model. This deviation is
388 more pronounced in solutions such as OKS that contain high [DOC] and occurs more frequently
389 with IP than AC, which correlated to higher rates of O₂ consumption as discussed above. This
390 occurred even though IP irradiations were consistently shorter in duration than AC (IP: ~8 hr,
391 AC: ~25 hr). Whatever the source of the O₂ depletion, further study of this phenomenon is
392 warranted, as the fundamental chemical reactivity of photosensitizers including ³DOM are
393 altered in the presence of lower DO (14, 18).

394 While we observed a strong correlation between DO depletion and spectral slope changes
395 over the experimental timeframes in this study, it can be argued that low-O₂ conditions may not
396 be representative of shallow wetland waters (assumed to be well-mixed and aerated at the top
397 layers where photoreactivity is most relevant). Comparative studies between closed and open
398 solar simulation experiments are needed in order to determine whether differences in the

399 mechanisms and rates of contaminant phototransformation exist and if they point to a preferred
400 set of photofate testing procedures in natural waters.

401 **Acknowledgements**

402 This study was supported by funding from the Ohio Water Development Authority grant
403 OWDA-4968, the National Science Foundation grants CBET-0504434 and CBET-1133094, and
404 the Ohio State University Environmental Science Graduate Program. Special thanks to Dr. Sue
405 Welch for nutrient analysis of water samples, Ross and Mary Yocom of Yocom Farm, Krispin
406 Fernandes, Clark Liu and Philip Moravcik of the University of Hawaii, Maya Wei-Haas for help
407 with the graphics, and Matthew Yin for statistical analysis and consultation.

408

409

References

- 410 1. Brinkmann T., Horsch P., Sartorius D., Frimmel F.H. 2003. Photoformation of low-
411 molecular-weight organic acids from brown water dissolved organic matter.
412 *Environmental Science and Technology* 37:4190-4198.
- 413 2. White E.M., Vaughan P.P., Zepp R.G. 2003. Role of the photo-Fenton reaction in the
414 production of hydroxyl radicals and photobleaching of colored dissolved organic matter
415 in a coastal river of the southeastern United States. *Aquatic Sciences* 65:402-414.
- 416 3. Vahatalo A.V., Salonen K., Sasaki E., Salkinoja-Salonen M.S. 2002. Bleaching of color of
417 kraft pulp mill effluents and natural organic matter in lakes. *Canadian Journal of*
418 *Fisheries and Aquatic Sciences* 59:808-818.
- 419 4. Andrews S.S., Caron S., Zafiriou O.C. 2000. Photochemical oxygen consumption in
420 marine waters: A major sink for colored dissolved organic matter? *Limnology and*
421 *Oceanography* 45:267-277.
- 422 5. Helms J.R., Stubbins A., Ritchie J.D., Minor E.C., Kieber D.J., Mopper K. 2008.
423 Absorption spectral slopes and slope ratios as indicators of molecular weight, source, and
424 photobleaching of chromophoric dissolved organic matter. *Limnology and Oceanography*
425 53:955-969.
- 426 6. Moran M.A., Sheldon W.M., Zepp R.G. 2000. Carbon loss and optical property changes
427 during long-term photochemical and biological degradation of estuarine dissolved
428 organic matter. *Limnology and Oceanography* 45:1254-1264.
- 429 7. Vahatalo A.V., Wetzel R.G. 2004. Photochemical and microbial decomposition of
430 chromophoric dissolved organic matter during long (months-years) exposures. *Marine*
431 *Chemistry* 89:313-326.
- 432 8. Cory R.M., McNeill K., Cotner J.P., Amado A., Purcell J.M., Marshall A.G. 2010.
433 Singlet Oxygen in the Coupled Photochemical and Biochemical Oxidation of Dissolved
434 Organic Matter. *Environmental Science and Technology* 44:3683-3689.
- 435 9. Vione D., Lauri V., Minero C., Maurino V., Malandrino M., Carlotti M.E., Olariu R-I.,
436 Arsene C. 2009. Photostability and photolability of dissolved organic matter upon
437 irradiation of natural water samples under simulated sunlight. *Aquatic Sciences* 71:34-45.
- 438 10. Lam M.W., Tantuco K., Mabury S.A. 2003. PhotoFate: A new approach in accounting
439 for the contribution of indirect photolysis of pesticides and pharmaceuticals in surface
440 waters. *Environmental Science and Technology* 37:899-907.
- 441 11. Brezonik P.L., Fulkerson-Brekken J. 1998. Nitrate-induced photolysis in natural waters:
442 Controls on concentrations of hydroxyl radical photo-intermediates by natural scavenging
443 agents. *Environmental Science and Technology* 32:3004-3010.
- 444 12. Gerecke A.C., Canonica S., Muller S.R., Scherer M., Schwarzenbach R.P. 2001.
445 Quantification of dissolved natural organic matter (DOM) mediated phototransformation
446 of phenylurea herbicides in lakes. *Environmental Science and Technology* 35:3915-3923.
- 447 13. Sulzberger B., Durisch-Kaiser E. 2009. Chemical characterization of dissolved organic
448 matter (DOM): A prerequisite for understanding UV-induced changes of DOM
449 absorption properties and bioavailability. *Aquatic Sciences* 71:104-126.
- 450 14. Sharpless C. M., Aeschbacher M., Page S. E., Wenk J., Sander M., and McNeill K. 2014.
451 Photooxidation-Induced Changes in Optical, Electrochemical and Photochemical

- 452 Properties of Humic Substances. *Environmental Science and Technology* ASAP, DOI:
453 10.1021/es403925g
- 454 15. Wallace D.F., Hand L.H., Oliver R.G. 2010. The role of indirect photolysis in limiting
455 the persistence of crop protection products in surface waters. *Environmental Toxicology*
456 *and Chemistry* 29:575-581.
- 457 16. Miller P.L., Chin Y.P. 2005. Indirect photolysis promoted by natural and engineered
458 wetland water constituents: Processes leading to alachlor degradation. *Environmental*
459 *Science and Technology* 39:4454-4462.
- 460 17. Halladja S., ter Halle A., Pilichowski J.F., Boulkamh A., Richard C. 2009. Fulvic acid-
461 mediated phototransformation of mecoprop. A pH-dependent reaction. *Photochemical*
462 *and Photobiological Sciences* 8:1066-1071.
- 463 18. Sharpless C.M. 2012. Lifetimes of Triplet Dissolved Natural Organic Matter (DOM) and
464 the Effect of NaBH₄ Reduction on Singlet Oxygen Quantum Yields: Implications for
465 DOM Photophysics. *Environmental Science and Technology* 46:4466-4473.
- 466 19. Canonica S., Laubscher H.U. 2008. Inhibitory effect of dissolved organic matter on
467 triplet-induced oxidation of aquatic contaminants. *Photochemical and Photobiological*
468 *Sciences* 7:547-551.
- 469 20. Wenk J., von Gunten U., Canonica S. 2011. Effect of Dissolved Organic Matter on the
470 Transformation of Contaminants Induced by Excited Triplet States and the Hydroxyl
471 Radical. *Environmental Science and Technology* 45:1334-1340.
- 472 21. Weishaar J.L., Aiken G.R., Bergamaschi B.A., Fram M.S., Fujii R., Mopper K. 2003.
473 Evaluation of specific ultraviolet absorbance as an indicator of the chemical composition
474 and reactivity of dissolved organic carbon. *Environmental Science and Technology*
475 37:4702-4708.
- 476 22. Miller P.L., Chin Y.P. 2002. Photoinduced degradation of carbaryl in a wetland surface
477 water. *Journal of Agricultural and Food Chemistry* 50:6758-6765.
- 478 23. Dulin D., Mill T. 1982. Development and evaluation of sunlight actinometers.
479 *Environmental Science and Technology* 16:815-820.
- 480 24. Leifer A. 1988. *The Kinetics Of Environmental Aquatic Photochemistry: Theory And*
481 *Practice*. American Chemical Society, Washington, DC.
- 482 25. Yamashita Y., Scinto L.J., Maie N., Jaffe R. 2010. Dissolved Organic Matter
483 Characteristics Across a Subtropical Wetland's Landscape: Application of Optical
484 Properties in the Assessment of Environmental Dynamics. *Ecosystems* 13:1006-1019.
- 485 26. Galgani L., Tognazzi A., Rossi C., Ricci M., Galvez J.A., Dattilo A.M., Cozar A.,
486 Bracchini L., Loïselle S.A. 2011. Assessing the optical changes in dissolved organic
487 matter in humic lakes by spectral slope distributions. *Journal of Photochemistry and*
488 *Photobiology B-Biology* 102:132-139.
- 489 27. Gao H.Z., Zepp R.G. 1998. Factors influencing photoreactions of dissolved organic
490 matter in a coastal river of the southeastern United States. *Environmental Science and*
491 *Technology* 32:2940-2946.
- 492 28. Haag W.R., Hoigne J. 1986. Singlet oxygen in surface waters 3. Photochemical formation
493 and steady-state concentrations in various types of waters. *Environmental Science and*
494 *Technology* 20:341-348.
- 495 29. Voelker B.M., Morel F.M.M., Sulzberger B. 1997. Iron redox cycling in surface waters:
496 Effects of humic substances and light. *Environmental Science and Technology* 31:1004-
497 1011.

- 498 30. Millet M., Palm W.U., Zetzsch C. 1998. Investigation of the photochemistry of urea
499 herbicides (chlorotoluron and isoproturon) and quantum yields using polychromatic
500 irradiation. *Environmental Toxicology and Chemistry* 17:258-264.
- 501 31. Wilson R.I., Mabury S.A. 2000. Photodegradation of metolachlor: Isolation,
502 identification, and quantification of monochloroacetic acid. *Journal of Agricultural and*
503 *Food Chemistry* 48:944-950.
- 504 32. Dimou A.D., Sakkas V.A., Albanis T.A. 2005. Metolachlor photodegradation study in
505 aqueous media under natural and simulated solar irradiation. *Journal of Agricultural and*
506 *Food Chemistry* 53:694-701.
- 507 33. Benitez F.J., Acero J.L., Real F.J., Maya C. 2004. Modeling of photooxidation of
508 acetamide herbicides in natural waters by UV radiation and the combinations UV/H₂O₂
509 and UV/O₃. *Journal of Chemical Technology and Biotechnology* 79:987-997.
- 510 34. Vione D., Falletti G., Maurino V., Minero C., Pelizzetti E., Malandrino M., Ajassa R.,
511 Olariu R., Arsene C. 2006. Sources and sinks of hydroxyl radicals upon irradiation of
512 natural water samples. *Environmental Science and Technology* 37:3775-3781.
- 513 35. Brekken J.F., Brezonik P.L. 1998. Indirect photolysis of acetochlor: Rate constant of a
514 nitrate-mediated hydroxyl radical reaction. *Chemosphere* 36:2699-2704.
- 515 36. Jacobs L.E., Fimmen R.L., Chin Y-P., Mash H.E., Weavers L.K. 2011. Fulvic acid
516 mediated photolysis of ibuprofen in water. *Water Research* 45:4449-4458.
- 517 37. Canonica S., Freiburghaus M. 2001. Electron-rich phenols for probing the photochemical
518 reactivity of freshwaters. *Environmental Science and Technology* 35:690-695.
- 519 38. Paul A., Stosser R., Zehl A., Zwirnmann E., Vogt R.D., Steinberg C.E.W. 2006. Nature
520 and abundance of organic radicals in natural organic matter: Effect of pH and irradiation.
521 *Environmental Science and Technology* 40:5897-5903.
- 522 39. Galichet F., Mailhot G., Bonnemoy F., Bohatier J., Bolte M. 2002. Iron(III) photo-
523 induced degradation of isoproturon: correlation between degradation and toxicity. *Pest*
524 *Management Science* 58:707-712.
- 525 40. Bruccoleri A., Pant B. C., Sharma D. K., and Langford C. H. 1993. Evaluation of primary
526 photoproduct quantum yields in fulvic acid. *Environmental Science and Technology* 27:
527 889-894.
- 528 41. Guerard J.J., Chin Y-P., Mash H., Hadad C.M. 2009. Photochemical Fate of
529 Sulfadimethoxine in Aquaculture Waters. *Environmental Science and Technology*
530 43:8587-8592.
- 531 42. Golanoski K.S., Fang S., Del Vecchio R., Blough N.V. 2012. Investigating the
532 Mechanism of Phenol Photooxidation by Humic Substances. *Environmental Science and*
533 *Technology* 46:3912-3920.
- 534 43. Canonica S., Hellrung B., Muller P., Wirz J. 2006. Aqueous oxidation of phenylurea
535 herbicides by triplet aromatic ketones. *Environmental Science and Technology* 40:6636-
536 6641.
- 537 44. Dalrymple R.M., Carfagno A.K., Sharpless C.M. 2010. Correlations between Dissolved
538 Organic Matter Optical Properties and Quantum Yields of Singlet Oxygen and Hydrogen
539 Peroxide. *Environmental Science and Technology* 44:5824-5829.
- 540 45. Goncalves C., Perez S., Osorio V., Petrovic M., Alpendurada M.F., Barcelo D. 2011.
541 Photofate of Oseltamivir (Tamiflu) and Oseltamivir Carboxylate under Natural and
542 Simulated Solar Irradiation: Kinetics, Identification of the Transformation Products, and
543 Environmental Occurrence. *Environmental Science and Technology* 45:4307-4314.

544 46. Weber J., Halsall C.J., Wargent J.J., Paul N.D. 2009. A comparative study on the aqueous
545 photodegradation of two organophosphorus pesticides under simulated and natural
546 sunlight. *Journal of Environmental Monitoring* 11:654-659.

547

548

549

550

551 **Table 1:** Chemical constituent concentrations and optical characterization of collected wetland
 552 water samples

Water Sample	Date collected	pH	[Fe _{tot}] (μM)	[NO ₃ /NO ₂] (μM N)	Total [N] (μM N)	[DOC] (mg C/L)	SUVA ₂₅₄ (M ⁻¹ cm ⁻¹)	SF ₍₂₉₀₋₃₇₀₎ ^a	S ₍₂₇₅₋₂₉₅₎ ^b	S ₍₃₅₀₋₄₀₀₎ ^b	S _R ^b
YCF	07/01/10	8.9	3.6	1.55	586	7.20 ± 0.2	372	0.921	0.015	0.015	1.02
KNM	12/18/10	6.1	29	bdl ^c	119	32.2 ± 0.2	221	0.780	0.012	0.015	0.81
EVG	12/31/10	7.9	1.1	0.68	118	25.0 ± 0.1	351	0.814	0.020	0.020	0.99
OKS _{FF}	01/01/11	3.5	4.3	2.64	73.7	52.5 ± 0.7	230	0.687	0.014	0.013	1.04
OKS _{LF}	01/01/11	3.5	6.8	7.50	510	139 ± 0.7	174	0.513	0.014	0.015	0.93

553
 554 ^a Screening factor calculated over $\lambda = 290-370$ nm.
 555 ^b Spectral slope of linearized UV-vis absorbance over the ranges $\lambda = 275-295$ nm, $\lambda = 350-400$
 556 nm, and the ratio of the two, after [5].
 557 ^c Below detection limit (~10 ppb N = 0.7 μM)
 558 EVG = Everglades water; OKS = Okefenokee Swamp water (LF = lab-filtered, FF = field-filtered);
 559 YCF = Yocom Farm water (Ohio)
 560

561

562

563 **Table 2:** Rates of change in optical characteristics and dissolved oxygen of wetland waters
 564 during irradiation

Wetland Waters	Rates of change of photobleaching parameters				Correlation between DO and spectral rates of change ^a		
	DO ^b	S ₂₇₅₋₂₉₅ ^c	S ₃₅₀₋₄₀₀ ^c	S _R ^d	S ₂₇₅₋₂₉₅	S ₃₅₀₋₄₀₀	S _R
EVG							
alone	-1.04 ± 0.3	1.08 ± 0.01	-0.263 ± 0.01	68.5 ± 0.1	0.81	0.74	0.87
AC only	-1.35 ± 0.3	1.34 ± 0.01	-0.303 ± 0.04	70.9 ± 0.2	0.83	0.14	0.93
IP only	-1.71 ± 0.1	0.94 ± 0.02	-1.77 ± 0.07	143 ± 0.5	0.36	0.45	0.46
AC, Low-O ₂	0	0.97 ± 0.03	-0.446 ± 0.04	74.1 ± 0.3	0.07	0.20	0.18
IP, Low-O ₂	0	1.09 ± 0.01	-0.463 ± 0.05	81.2 ± 0.2	0.03	0.00	0.06
AC, t-butanol	-1.06 ± 0.3	1.42 ± 0.01	0.348 ± 0.01	52.0 ± 0.1	0.93	0.72	0.95
OKS _{FF}							
AC only	-2.96 ± 1.0	1.78 ± 0.02	1.07 ± 0.04	43.7 ± 0.1	0.74	0.77	0.55
IP only	-5.76 ± 1.4	2.10 ± 0.02	0.033 ± 0.01	83.0 ± 0.1	-	-	-
OKS _{LF}							
AC only	-3.74 ± 1.7	1.32 ± 0.02	1.14 ± 0.03	15.1 ± 0.1	0.70	0.80	0.08
IP only	-9.42 ± 1.6	2.63 ± 0.04	2.34 ± 0.03	29.4 ± 0.1	0.97	0.96	0.97

565

566 ^a Coefficient of determination (R²) for rates of change of spectral parameters (S) indicated as
 567 function of DO.

568 ^b Rate of change of DO (x 10⁻² % hr⁻¹) compared to 100% atmospheric saturation.

569 ^c Rate of change of spectral slope (S) region indicated (x 10⁻³ hr⁻¹)

570 ^d Rate of change of spectral slope (S) ratio (x 10⁻² hr⁻¹)

571 AC = Acetochlor (5 μM); DO = Dissolved oxygen; EVG = Everglades water; IP = Isoproturon
 572 (5 μM); OKS = Okefenokee Swamp water (LF = lab-filtered, FF = field-filtered)

573 Errors represent 95% confidence intervals.

574

575 **Table 3:** Reaction rate constants for the photodegradation of AC and IP in various waters under
 576 simulated sunlight

Water Sample	k_{obs} ($\cdot 10^{-2}$ hr $^{-1}$) ^a		k_{dir} ($\cdot 10^{-2}$ hr $^{-1}$) ^b		k_{ind} ($\cdot 10^{-2}$ hr $^{-1}$) ^c	
<i>Wetland Waters</i> ^d	<i>AC</i>	<i>IP</i>	<i>AC</i>	<i>IP</i>	<i>AC</i>	<i>IP</i>
YCF	1.9 ± 0.1	12.7 ± 0.4	0.69 ± 0.06	0.25 ± 0.09	1.2 ± 0.1	12.4 ± 0.8
KNM	1.6 ± 0.1	16.4 ± 0.9	0.58 ± 0.06	0.21 ± 0.09	1.0 ± 0.1	16.2 ± 0.7
EVG	1.8 ± 0.1	30 ± 3.0	0.61 ± 0.06	0.22 ± 0.09	1.2 ± 0.2	30 ± 2.0
OKS _{FF}	5.4 ± 0.5	6.7 ± 0.7	0.51 ± 0.06	0.19 ± 0.09	4.9 ± 0.5	6.5 ± 0.7
OKS _{LF}	1.7 ± 0.1	4.1 ± 0.4	0.38 ± 0.06	0.14 ± 0.09	1.3 ± 0.1	3.9 ± 0.4
<i>PLFA</i> ^e						
7 mg C/L	1.6 ± 0.1	20.6 ± 1.8	0.75 ± 0.06	0.27 ± 0.09	0.9 ± 0.1	20 ± 2.0
14 mg C/L	2.0 ± 0.2	25.5 ± 3.3	0.75 ± 0.06	0.27 ± 0.09	1.2 ± 0.2	25 ± 3.0
21 mg C/L	2.2 ± 0.1	31.9 ± 3.7	0.75 ± 0.06	0.27 ± 0.09	1.4 ± 0.1	32 ± 4.0

577 ^a Observed experimental reaction rate constant

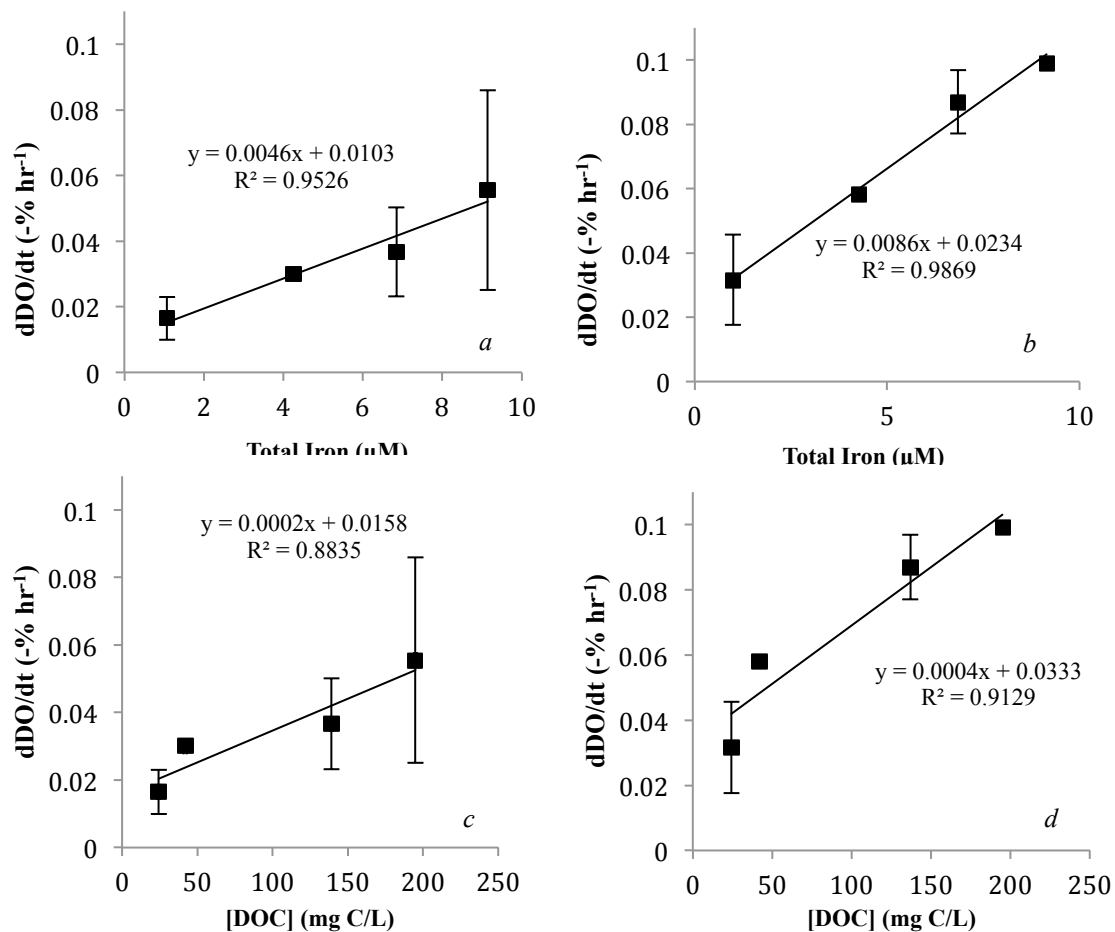
578 ^b Direct photolysis rate constant corrected for light screening by $k_{UP} \cdot SF_{290-370}$; where $k_{UP, AC} =$
 579 $7.5 \pm 0.6 \times 10^{-3}$ hr $^{-1}$; $k_{UP, IP} = 2.7 \pm 0.9 \times 10^{-3}$ hr $^{-1}$

580 ^c Indirect photolysis rate constant $k_{ind} = k_{obs} - k_{dir}$

581 ^d Unless otherwise noted, experimental conditions: field pH, atmospheric gas saturation before
 582 photolysis, 5 μ M herbicide

583 ^e Fulvic acid solutions diluted from stock solution, distinguished by final [DOC]

584 AC = Acetochlor (5 μ M); EVG = Everglades water; IP = Isoproturon (5 μ M); OKS =
 585 Okefenokee Swamp water (LF = lab-filtered, FF = field-filtered); YCF = Yocom Farm water
 586 (Ohio)



587

588

589

590

591

592

593

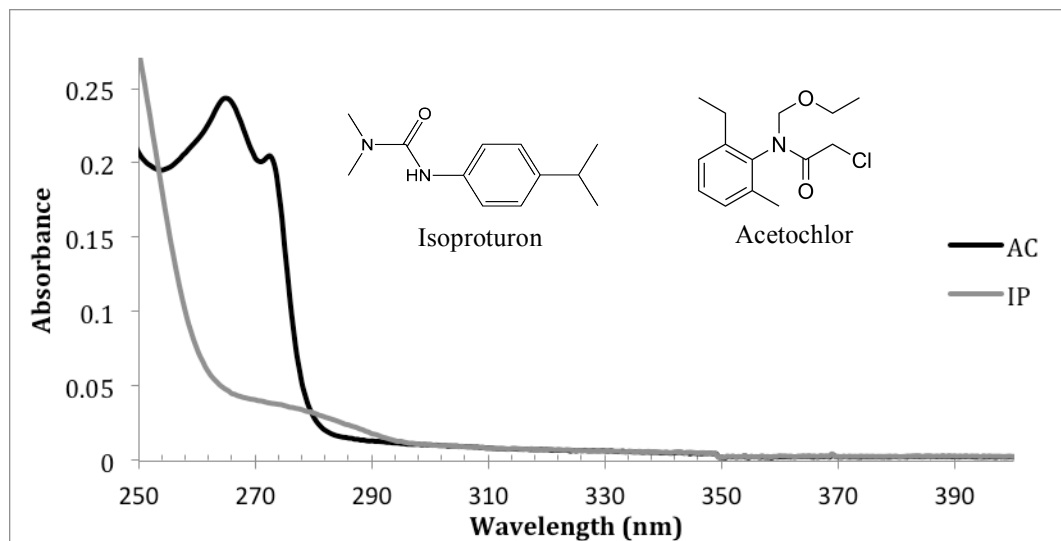
594

595

Figure 1: DO loss rate as a function of concentration of dissolved organic carbon ([DOC]) or total iron ([Fe]) in irradiated wetland waters spiked with either acetochlor (AC; a, c) or isoproturon (IP; b, d). Points represent average of all trials. Error bars indicate standard deviation. Samples stored in acidified conditions, but brought to field pH for experiment were included in this regression (6 acidified out of 19 total) to have access to more points.

595

596

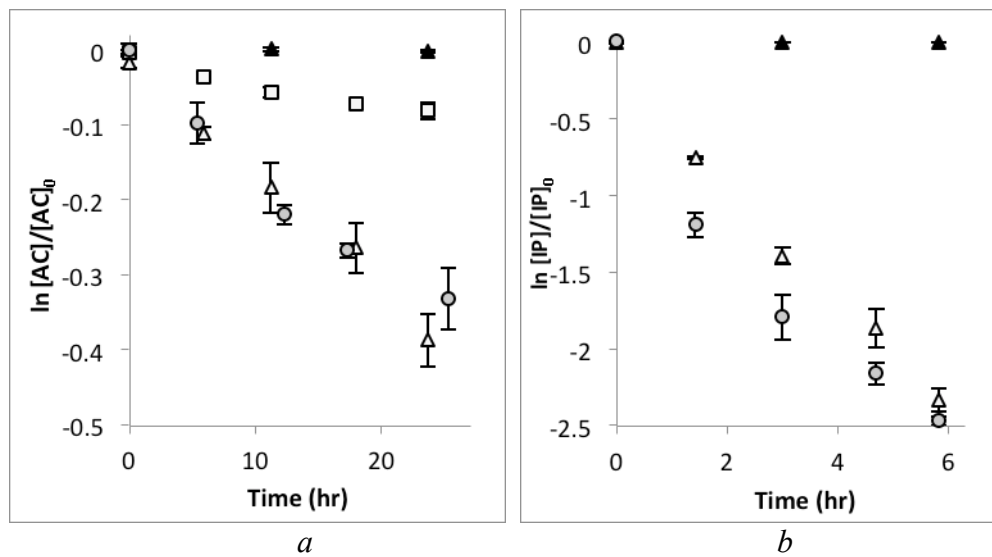


597

598

599 **Figure 2:** UV-visible absorbance spectra and chemical structures for the herbicides acetochlor
600 (AC; black line) and isoproturon (IP; gray line).

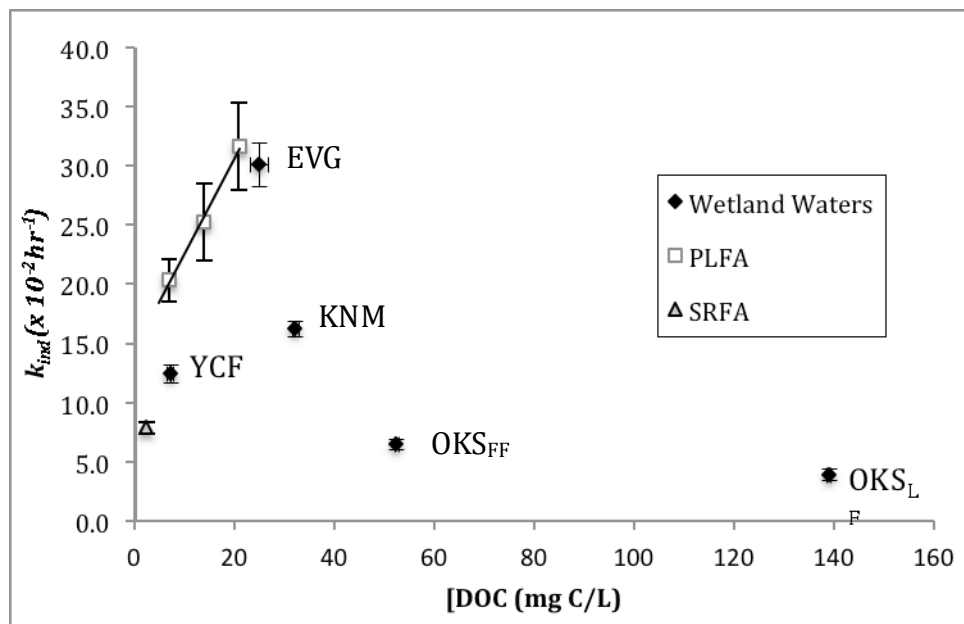
601



602
603
604
605
606
607
608
609

Figure 3: Change in herbicide concentrations (a: acetochlor, AC b: isoproturon, IP) during light exposure in Everglades (EVG) water under three conditions: standard (equilibrated in air, Δ), low- O_2 (\bullet), or with 25 mM t-butanol (AC only, \square). Dark symbols indicate dark controls. Error bars represent 95% confidence interval.

610



611
612
613
614
615
616
617

Figure 4: Indirect photolysis reaction rate constants for isoproturon (IP) as a function of dissolved organic carbon concentration ([DOC]) in various wetland waters (filled markers; field pH, see Table 1) and fulvic acid solutions (open markers, Δ = Suwannee River FA, \square = Pony Lake FA; pH = 8.0). Error bars represent 95% confidence interval.

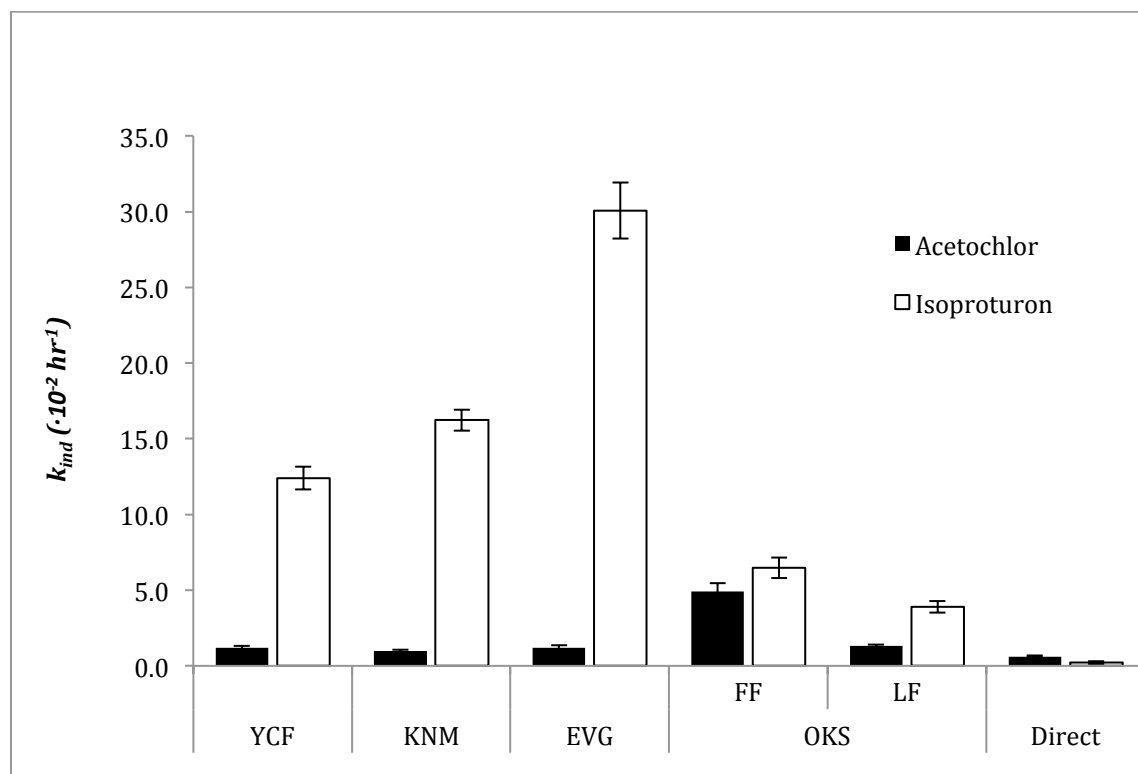


Figure 5: Indirect photolysis reaction rates (k_{ind}) for isoproturon and acetochlor in wetland water samples used in this study.